International Journal of Mechanical, Industrial and Aerospace Sciences
ISSN: 2517-9950
Vol:13, No:9, 2019

Investigation of Flow Characteristics on Upstream and Downstream of Orifice Using Computational Fluid Dynamics

War War Min Swe, Aung Myat Thu, Khin Cho Thet, Zaw Moe Htet, Thuzar Mon

***Abstract*—**The main parameter of the orifice hole diameter was designed according to the range of throttle diameter ratio which gave the required discharge coefficient. The discharge coefficient is determined by difference diameter ratios. The value of discharge coefficient is 0.958 occurred at throttle diameter ratio 0.5. The throttle hole diameter is 80 mm. The flow analysis is done numerically using ANSYS 17.0, computational fluid dynamics. The flow velocity was analyzed in the upstream and downstream of the orifice meter. The downstream velocity of non-standard orifice meter is 2.5% greater than that of standard orifice meter. The differential pressure is 515.379 Pa in standard orifice.

***Keywords*—**CFD-CFX, discharge coefficients, flow characteristics, inclined.

I. Introduction

THE orifice meter is the most widely used conventional differential pressure flow meter [1]. The main design specifications for orifice plates according to ISO 5167 covered the orifice plate of the circulatory bore, the flatness, the pressure tapping [2]. Husain and Teyssandier measured the shift in discharge coefficient using an unbeveled orifice plate a 6 inches flange-tapped orifice meter which has plate thickness 3.2 mm [3]. Husain and Goodson took data in 2 inches pipes with plate thickness 3.57 mm that are on the maximum limit in ISO 5167; it did not significantly change its discharge coefficient [3]. When it was beveled with e = 0.79 mm, larger shifts were occurred [3]. Morrison et al. observed that the effects of the upstream velocity profile upon the performance of orifice flowmeters. He observed that non-swirling maldistributed axial velocity profiles increasing the flow along the centerline of the pipe decreased the pressure drop across the orifice plate and resulted in increased discharge coefficients [4]. Martin analyzed the type of disturbances created by pipe fitting and valves and their effects on the performance of the orifice meter [5]. Irving calculated the discharge coefficient for upstream disturbed flow and different pressure tappings. He observed that the errors in measurement are less sensitive to flow disturbance, and subsequently recommended the use of standard tappings to ratify the errors in the flow measurements [6]. Singh et al. have proposed the design of a self-adjusting the variable area orifice meter with conical body. Husain and Goodson have reported the effect of the plate thickness and bevel angle on the discharge coefficient of the orifice diameter having 50 mm pipe diameter [7]. Kim et al. observed the significant effects of the plate thickness on the performance of the orifice meter at low diameter ratio ($\beta = 0.10$), but at higher β, no significant conclusions were drawn [8]. Singh had studied the performance of the orifice plate at non-standard condition [9]. He observed that at lower β values, the discharge coefficient of an orifice meter decreases marginally with increase in plate thickness [9]. The value of the discharge coefficient was altered for the plate thickness beyond 7.0 mm [9]. He observed that the bevel angle of an orifice plate has marginal impact on the discharge coefficient of office plate for difference plate thickness [9].

The objectives of the paper are to design the orifice hole which meets the differential pressure in the upstream and downstream of an orifice. The downstream velocity of an orifice will support to reach the required tunnel flow. An orifice meter mention in this paper is one of the components of the wind tunnel assembly. The parameters of wind tunnel assembly were used for this paper [10]. The wind tunnel is useful in performance test of aerodynamic filed such as turbomachinery. The crucial characteristics of a wind tunnel are the flow quality inside the test chamber and the overall performances. The main purpose of this paper is to detect the flow velocity and the differential pressure in the upstream and downstream of the orifice meter. Thus, an orifice diameter is calculated with respect to diameter ratio $\boldsymbol{\beta}$. The orifice diameter is modified with the bevel 45°. The flow characteristics are analyzed in the upstream and downstream of the orifice meter by numerically using ANSYS 17.0 (CFD-CFX).

II. Geometry of Wind Tunnel

A. Geometry and Component of Wind Tunnel

The components and geometries of wind tunnel are described as shown in Fig. 1. The size of the wind tunnel is 3000×1800×1800 mm^3 [10]. The orifice meter plate is fitted 1800 mm apart from the ground. The diameter of the duct is 152.4 mm. The axial fan is setup 2900 mm apart from the ground. The volume flow rate of axial fan is 0.135 m^3/s (1875 m^3/hr) and it rotates 2500 rpm. The flow direction starting from axial fan to the wind tunnel is shown in Fig. 1.

B. Orifice Design

To design an orifice throttle diameter according to the throttle diameter ratio β, the specification parameter of mass

War War Min Swe is with the Mandalay Technological University, Pathein Gyi Township, Myanmar (phone: +95 9401559469, e-mail: warwarminswe@mtu.edu.mm).

flow rates, the density and the expansibility factor of air at 25° C are listed in Table I.

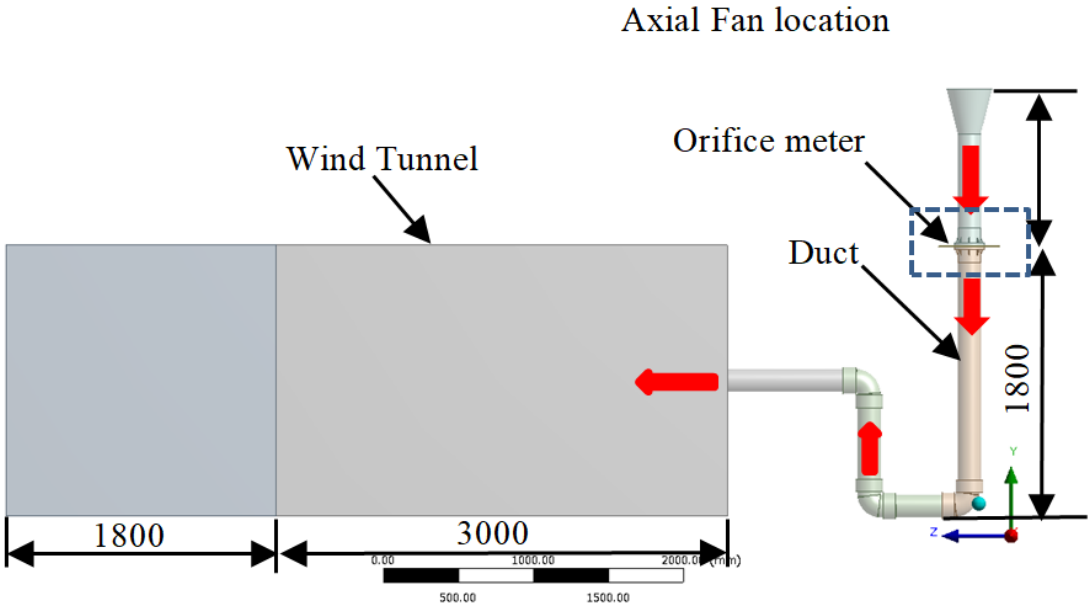

Fig. 1 Wind Tunnel Assembly

The dimensionless parameter Reynolds number, tapping location and tapping diameter are calculated using (1)-(3):

$$R_e = \frac{u_i d}{\nu} \tag{1}$$

$$A = \left(\frac{19000\beta}{R_{e_D}} \right)^{0.8} \tag{2}$$

$$M_2' = \frac{2L_1}{1-\beta} \tag{3}$$

The discharge coefficient (C) and the desired range of differential pressures are calculated using (4) and (5):

$$\begin{aligned} C = {} & 0.5961 + 0.0261\beta^2 - 0.261\beta^8 + 0.000521\left(\frac{10^6\beta}{R_{e_D}} \right)^{0.7} \\ & + \left(0.0188 + 0.0063A^{0.8}\right)\beta^{3.5}\left(\frac{10^6\beta}{R_{e_D}} \right)^{0.3} \\ & + \left(0.043 + 0.080e^{-10L_1} - 0.123e^{-7L1}\right) + (1 - 0.11A)\left(\frac{\beta^4}{1-\beta^4} \right) \\ & - 0.031\left(M_2' - 0.8M_2'^{1.1} \right)\beta^{1.3} \end{aligned} \tag{4}$$

$$Q = \frac{C\,\varepsilon\,F_r}{\sqrt{1-\beta^4}} \sqrt{\frac{2(P_1 - P_2)}{\rho}} \tag{5}$$

A flange tap is used as a method of extracting pressure. Fig. 2 shows the installation position of the flange tap. The pressure outlet on the upstream side of orifice plate is installed in the position, L_1 and the downstream side of the orifice plate is installed in the position, L_2.

TABLE I
SPECIFICATION DATA

Symbol	Quantity	Dimensions
β	throttle diameter ratio	0.2–0.6
ρ	density of air at 25°C	1.184 kg/m^3
ε	expansion coefficient of air at 25°C	1.0132
Q	volumetric flow rate of axial fan (Model: TSK 315)	1875 m^3/hr
D	diameter of duct	152.4 mm
ν	viscosity of air at 25°C	18.6×10^{-6}

TABLE II
RESULT FOR ORIFICE DIFFERENTIAL PRESSURES

Q (m^3/s)	ΔP = P_1 -P_2 (Pa)				
	$\beta = 0.2$	$\beta = 0.3$	$\beta = 0.4$	$\beta = 0.5$	$\beta = 0.6$
0.007	154.509	23.997	5.816	1.615	0.444
0.066	11660.012	1810.952	438.938	121.861	3.485
0.104	29025.161	4507.987	1092.643	303.347	83.353
0.135	49313.037	7658.959	1856.374	515.379	141.614
0.148	59092.021	9177.764	2224.501	617.581	169.697

III. THEORETICAL ANALYSIS RESULTS

The differential pressure is calibrated according to the range of throttle diameter ratio, β = 0.2–0.6 and the difference volume flow rates. The throttle diameter ratio, $\beta = 0.5$ and the volume flow rate 0.135 m^3/s gives the required differential pressure ΔP = 515.379 Pa (see Table II) and the throttle diameter, tapping diameter, d = 80 mm. The tapping location L_1

and L_2 is 24.6 mm respectively. The shape of the hole is circular and it is concentric with respect to the duct axis. The discharge coefficient, C=0.958 is observed *β=0.5*.

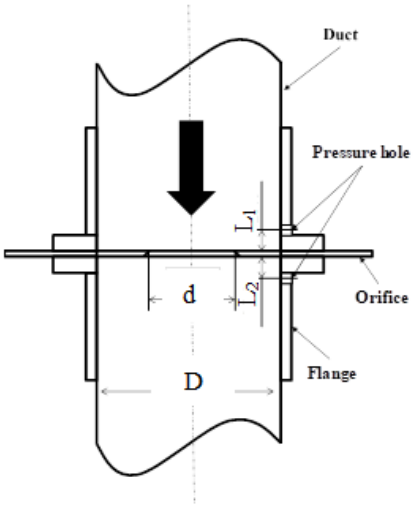

Fig. 2 An orifice with throttle

IV. Numerical Analysis

A. Geometry Orifice Assembly

An orifice assembly geometry is shown in Fig. 3. The throttle hole diameter is plotted according to the result of 80 mm in $\beta = 0.5$ (see Fig. 4). The plate thickness is 3.5 mm according to ISO 5167.

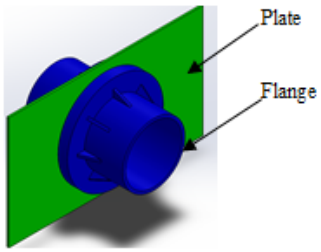

Fig. 3 Geometry of orifice assembly

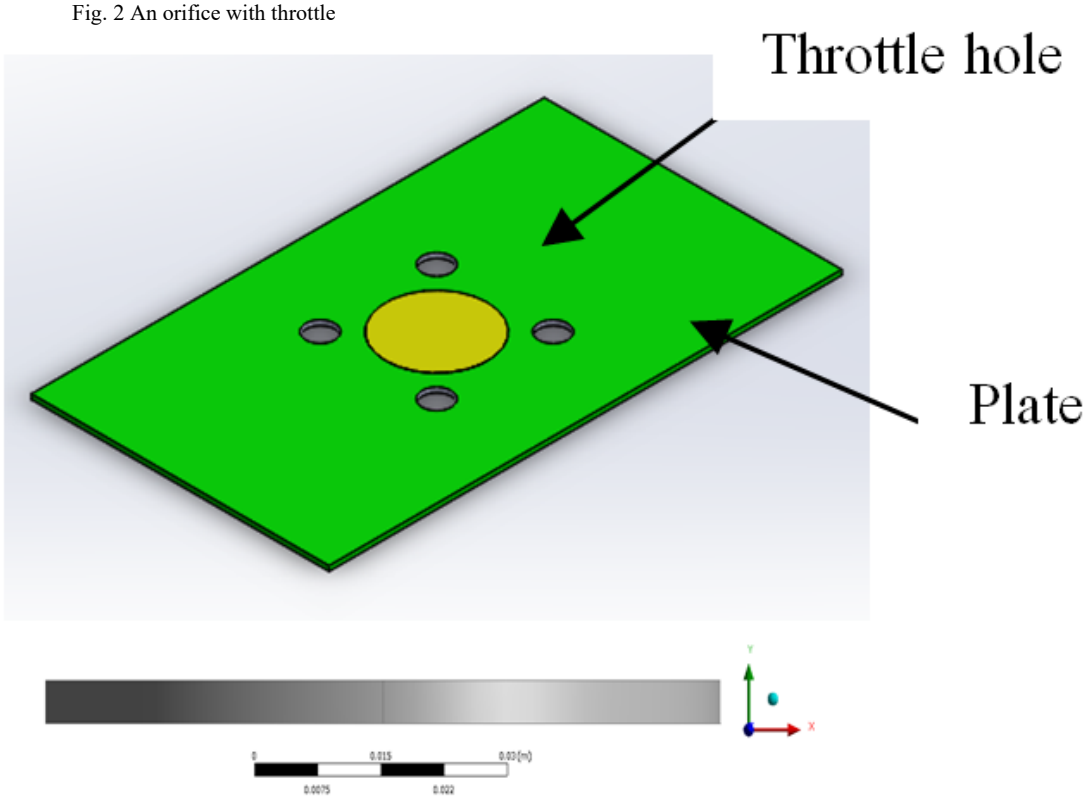

Fig. 4 Geometry of orifice assembly

B. Setup Procedure for Numerical Simulation

The numerical simulation is carried out according to the following step. ANSYS 17.0 software packet is used for this simulation. The flow analysis simulation for all contents: a design orifice with throttle diameter 80 mm and an orifice with modified throttle bevel 45° is carried out with computational fluid dynamic (CFD-CFX). There are five setup procedures for doing simulation (see Fig. 5).

The geometrical setup procedure mainly consists of the domains which pass through the working fluid. In this case, there are six domains (see Fig. 1). The enlarged view of the orifice section is mainly discussed for this simulation (see Fig.

6).

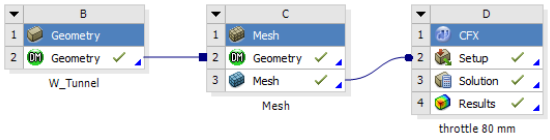

Fig. 5 Setup procedure for simulation

The orifice geometry with throttle hole diameter 80 mm and modified throttle bevel 45° is shown in Figs. 7 and 8. The total plate thickness is 3.5 mm. For modified throttle orifice, 1 mm is straight and the left 2.5 mm is the bevel 45 °C to the downstream.

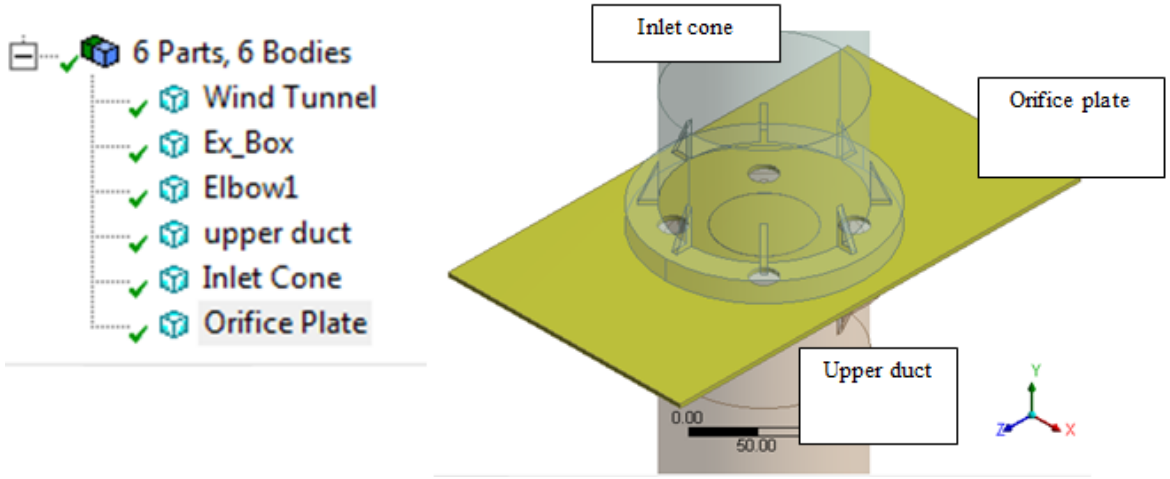

Fig. 6 Domain of orifice section

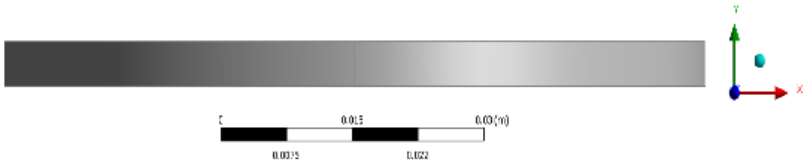

Fig. 7 Throttle hole of standard orifice

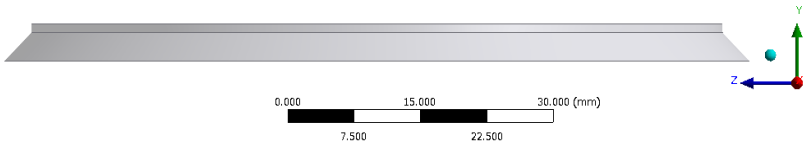

Fig. 8 Modified throttle hole with bevel 45°

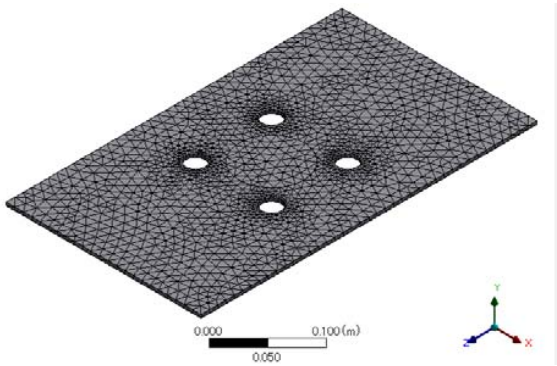

Fig. 9 Mesh in orifice domain

The domains are generated with the tetrahedron mesh. The total number of mesh is 4643434 and the total number of nodes is 823791. The maximum face size is 0.037 m and the minimum face size is 0.0037 m. The maximum Tet size is 0.74 m. The number of elements in orifice plate domain is 8780 and the number of node is 3039 (see Fig. 9).

The setup includes the following boundary conditions (see Table III and Fig. 10). In this simulation, two-equation turbulence models are used, as they offer a good compromise between numerical effort and computational accuracy. Both the velocity and length scale of turbulent are solved using separate transport equations (hence the term 'two-equation'). For numerical simulation, the *k-ω* based SST model is used. This model gives highly accurate predictions of the onset and the

amount of flow separation under adverse pressure gradients. The inlet boundary set mass flow rate, 0.175 kg/s, is calculated from the volume flow rate of axial fan (model: TSK 315). The outlet domain sets the average static pressure (0) Pa.

TABLE III
BOUNDARY CONDITIONS

Quantity	Boundary
analysis type	steady state
domain type	fluid
working fluid	air at 25°C
fluid model	turbulence, shear stress transport
inlet boundary	mass flow rate
outlet boundary	average static pressure
mass and momentum	no slip wall
wall roughness	smooth wall

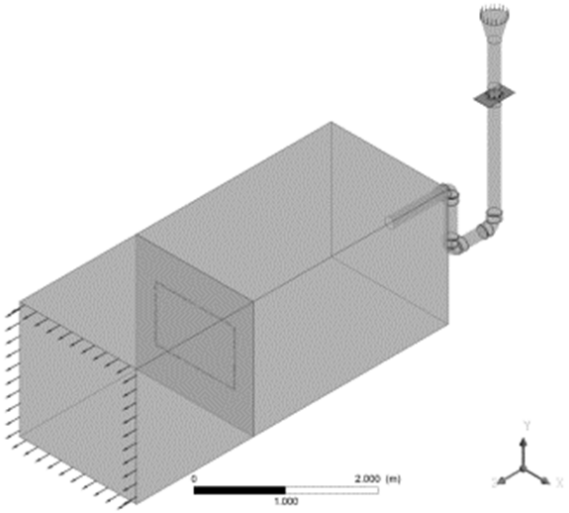

(a) Whole assembly

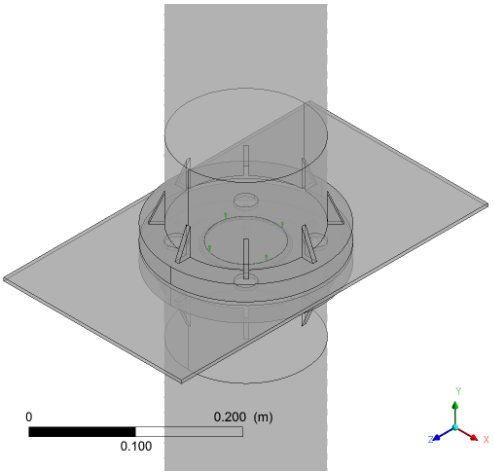

(b) Enlarge view of an orifice section

Fig. 10 Setup boundary condition

The RANS equations are solved iteratively. For each iteration, the errors, or residuals are reported as a measure of the overall conservation of the flow properties. Residual target was set $1\times E^{-4}$.

The final step is result. In CFD post screen, the simulation result of air velocity, the total pressure and velocity streamline on upstream and downstream of orifice meter are analyzed using contour, vector and streamline.

V. Result for Flow Characteristics

The upstream and downstream velocity of an orifice meter and modified orifice meter are plotted with contour in CFD-Post (see Figs. 11 and 12). The contour is plotted in the tapping location L_1 and L_2 ($L_1 = L_2 = 24.6$ mm).

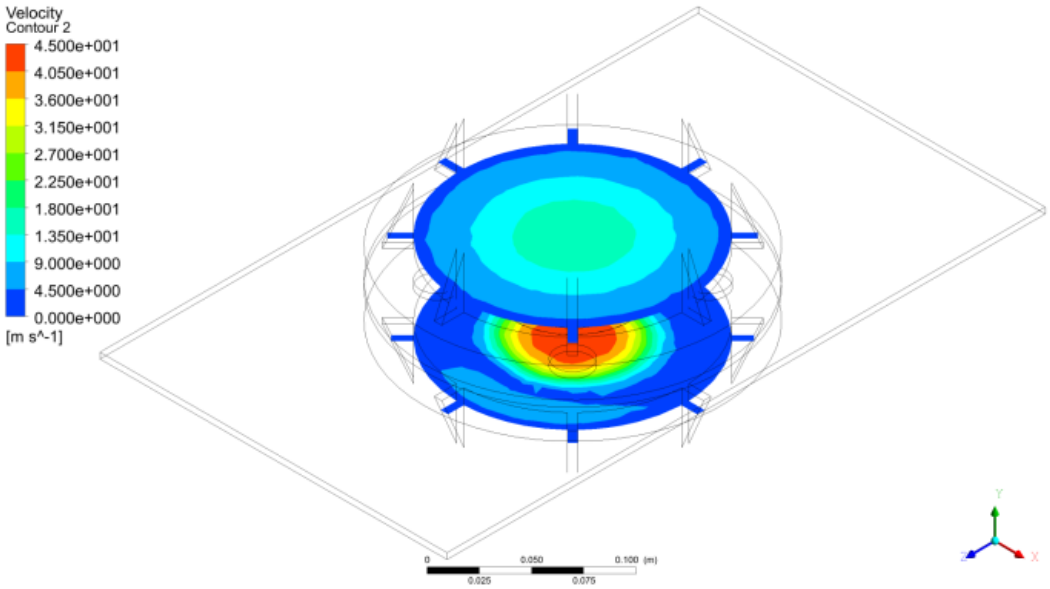

Fig. 11 Velocity contour upstream and downstream of standard orifice meter

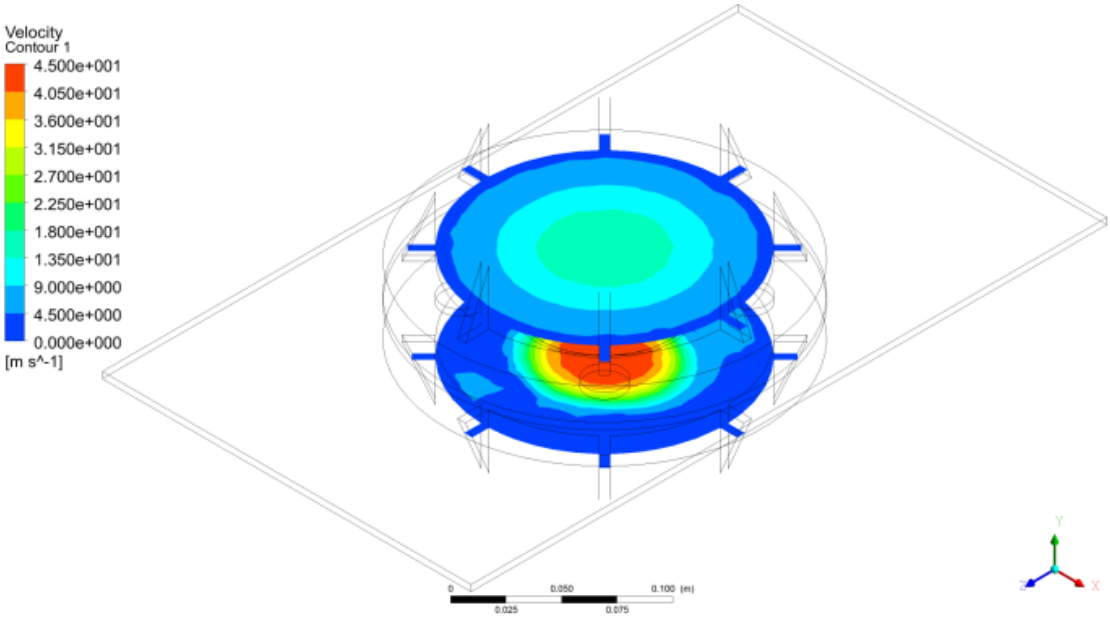

Fig. 12 Velocity contour upstream and downstream of modified orifice meter

The flow pattern is big difference on the upstream and the downstream of the orifices (see Figs. 11 and 12). The downstream velocity is higher than upstream velocity. The highest velocity is occurred in the axis of the tapping hole. The lowest velocity occurred near the wall of the duct.

The upstream flow velocity pattern is almost the same in the two cases (see Fig. 13). The downstream flow pattern is slightly different in the two cases (see Fig 14). It is clear in the axis of the duct. The recirculating flow occurs in the downstream of an orifice meter (see Fig. 15), but it does not occur in the downstream of modified orifice meter (see Fig. 16). The upstream flow pattern is uniform for the two cases.

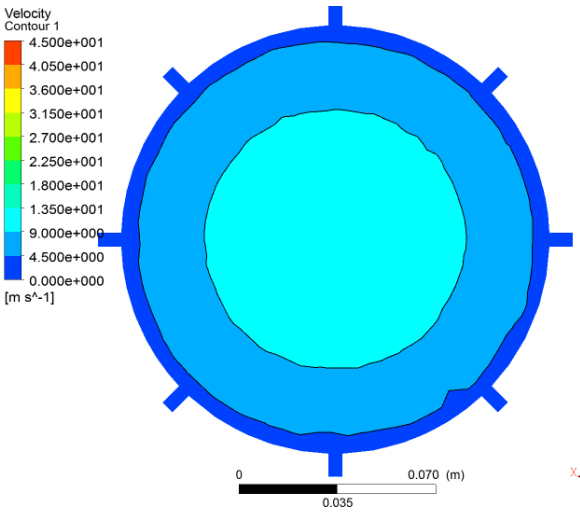

(a) Standard orifice meter

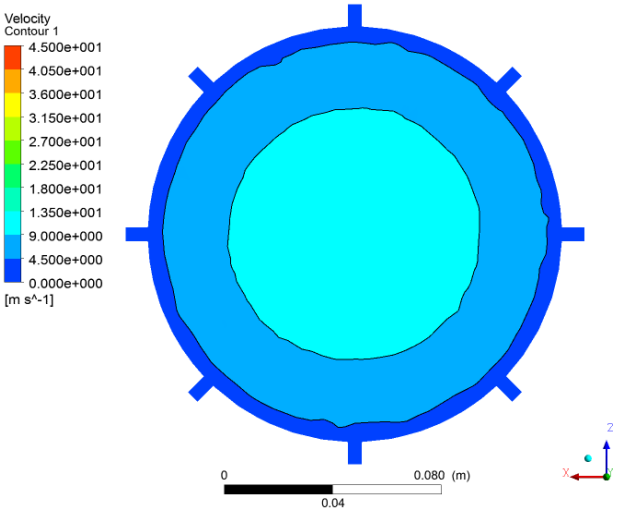

(b) Modified orifice meter with bevel 45°

Fig. 13 Upstream velocity contour

VI. Result for Velocity and Differential Pressure Analysis

The velocities are calibrated in the downstream of orifice meter. The velocity data are calibrated on the plane of contour from the left side of orifice meter to the right side of the orifice meter. The left side and the right of the velocity are lower than the velocity in the axis of orifice meter. The maximum velocity of standard orifice meter is about 43 m/s and that of the non-standard orifice meter is about 45 m/s (see Fig. 17).

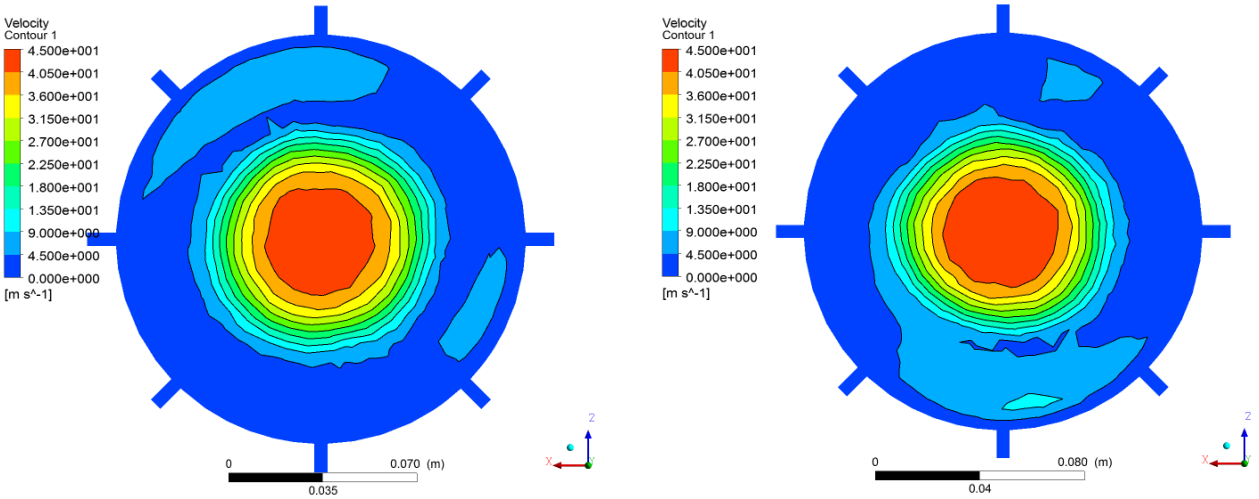

(a) Standard orifice meter

(b) Modified orifice meter with bevel 45°

Fig. 14 Downstream velocity contour

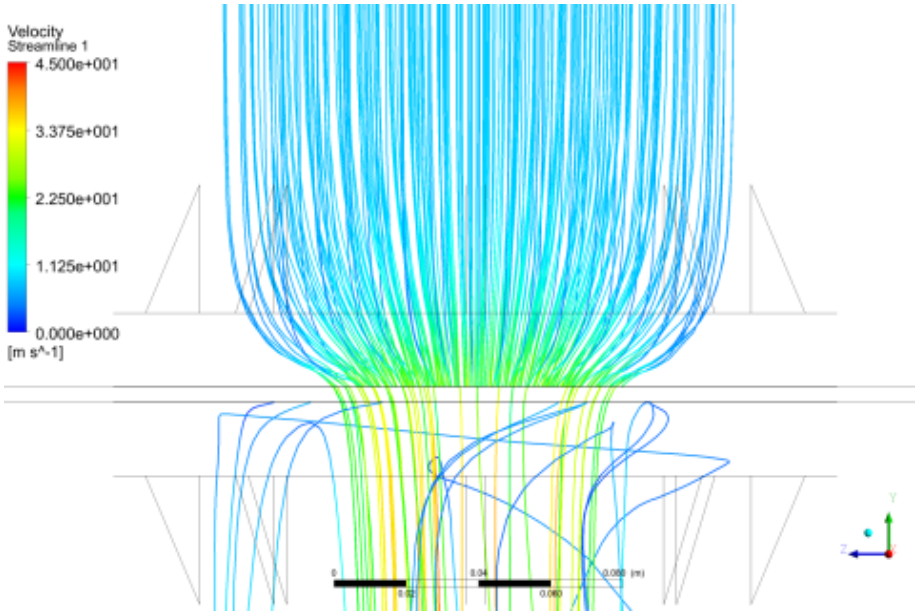

Fig. 15 Velocity streamline in standard orifice meter

The downstream velocity of modified bevel orifice meter (non-standard) is 2.5% greater than that of the velocity in standard orifice meter. The upstream velocity is almost the same for the two cases (see Fig. 17).

The upstream velocity of the orifices meter for two cases is almost the same. The minimum velocity is about 3.7 m/s and the maximum velocity is 16.41 m/s (see Fig. 18).

The differential pressure of downstream and upstream is calculated using (6). V_d is downstream velocity and V_u is upstream velocity of orifice meter.

$$\Delta P = \frac{1}{2}\rho_{air}\left(V_d^2 - V_u^2\right) \tag{6}$$

The value of differential pressure is 512.59 Pa for non-standard bevel orifice and the value is 490.2455 Pa for standard orifice. The differential pressure of non-standard orifice meter is greater 6.72% than the differential pressure of standard orifice.

VII. Conclusion

The differential pressure of non-standard orifices meter is greater than that of standard orifice meter. The downstream velocity of non-standard orifice meter (45°bevel) is greater than that of the standard orifice meter. The uniform flow pattern occurs in the upstream of the orifice meter. In the axis of non-standard orifice meter, the downstream velocity is greater about

63% than that of the upstream velocity. In the axis of standard orifice meter, the downstream velocity is greater about 60% than that of the upstream velocity.

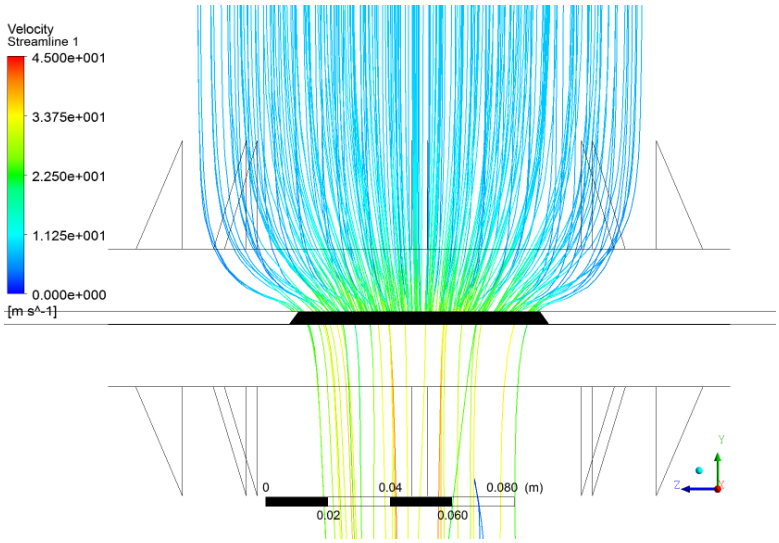

Fig. 16 Velocity streamline in modified orifice meter

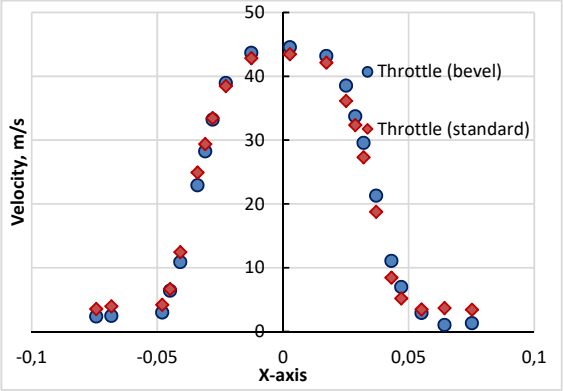

Fig. 17 Comparison of the velocity at downstream of standard and modified orifice meter

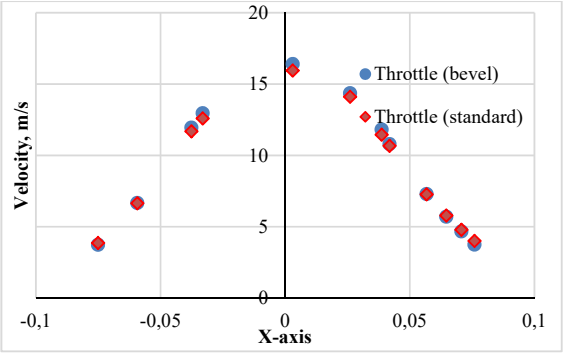

Fig. 18 Comparison of the velocity at upstream of standard and modified orifice meter

ACKNOWLEDGMENT

The author would like to thank JICA-EEHE organization. They supported and encouraged during the research work for promoting higher education.

REFERENCES

[1] W. R. Miller, *Flow measurement engineering hand book*, 3rd ed, New York: McGraw-Hill, 1996.
[2] M. Reader-Harris, "Orifice Plates and Venturi Tube", ISBN 978-3-319-16879-1, http://www.springer.com/978-3-319-16879-1, 2015
[3] M. Reader-Harris, J A Sattary & E P Spearman, "Flow Measurement Instrumentation," 6,(2), (1995)101.
[4] G. L. Morrison, K.R Hall, M.L. Macek, "Upstream Velocity Profile effects on orifice flowmeters," Flow Meas. Instrum., 2 (5), (1994) 92
[5] C N B Martin, "Int J Heat Fluid Flow", 3(3)(1982)135-141.
[6] J S Irving, "Int J Heat Fluidd Flow," *1(1)(1979)5-11.*
[7] S N Singh, B K Gandhi, V Seshadi & V S Chauhan, "Flow Meas Instrum",15 (2)92004)97-103.
[8] Z D Husain & F D Goodsan, "(ASME, Montvillargenne, Fr,1986),p. des Milieus poreux.; Ecole des Mines de Paris, Paris, Fr,1986''
[9] R K Singh,S N Singh & V Seshadri, "Performance evaluation of orifice plate assemblies under non-standard conditions using CFD",5(10)(2010).
[10] War War Min Swe, "*Aerodynamic Performance of Backward Centrifugal Fan with Rectangular Casing*," Ph.D Dissertation, Graduate School of Engineering Nagasaki University, 2017.